Volume 10 | Number 11 | 7 June 2023

10 YEARS ANNIVERSARY

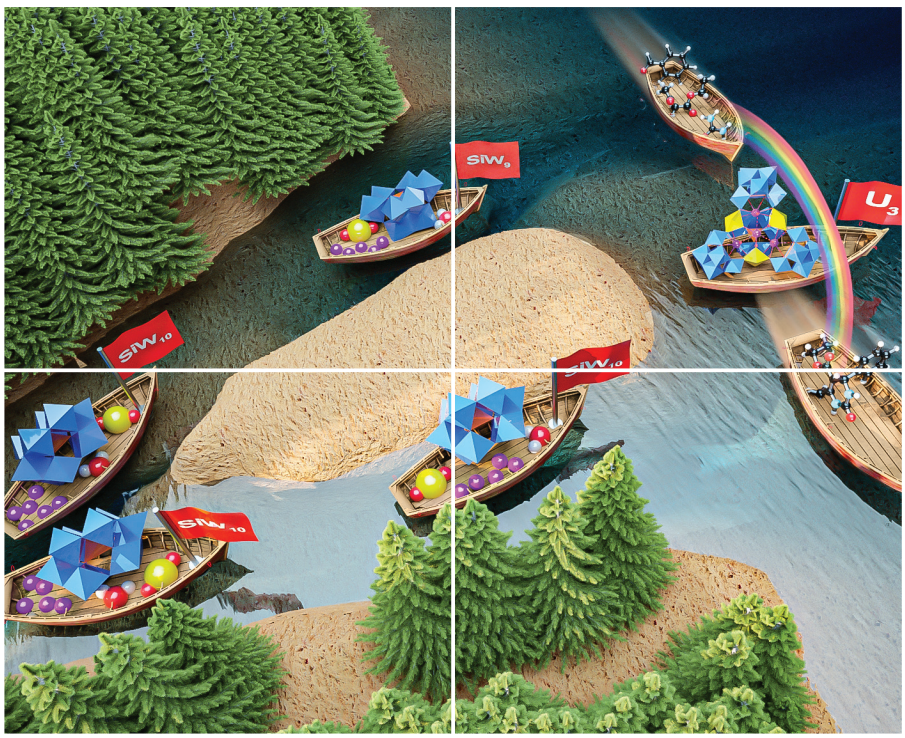

INORGANIC CHEMISTRY

FRONTIERS

CCS 中国化学会 CHINESE CHEMICAL SOCIETY
PEKING UNIVERSITY 1898
ROYAL SOCIETY OF CHEMISTRY
rsc.li/frontiers-inorganic

INORGANIC CHEMISTRY FRONTIERS

RESEARCH ARTICLE

View Article Online
View Journal | View Issue

Check for updates

Cite this: *Inorg. Chem. Front.*, 2023, **10**, 3195

Uranyl-silicotungstate-containing hybrid building units {α-SiW_9} and {γ-SiW_{10}} with excellent catalytic activities in the three-component synthesis of dihydropyrimidin-2(1*H*)-ones†

Jian-Hua Ding,‡[a] Yu-Feng Liu,‡[a] Zhao-Teng Tian,[a] Pei-Jie Lin,[a] Feng Yang,[c] Ke Li, *[a] Guo-Ping Yang *[a,b] and Yong-Ge Wei *[b]

Received 13th December 2022,
Accepted 28th January 2023

DOI: 10.1039/d2qi02653h

rsc.li/frontiers-inorganic

A novel uranyl-containing polytungstate, {$K_{4.2}Na_{18.9}H_{0.9}(H_2O)_{20}[K_4(UO_2)_3(H_2O)_6(\alpha\text{-}SiW_9O_{34})(\gamma\text{-}SiW_{10}O_{36})_3]$}·ca.$16H_2O$ (**U_3**), was synthesized using the Keggin-type precursor [γ-$SiW_{10}O_{36}$]$^{8-}$ ({γ-SiW_{10}}) and $UO_2(OAc)_2$ and was further characterized by single-crystal X-ray diffraction and various techniques. Single crystal X-ray diffraction analysis showed a quadrahedron-like structure of **U_3** with interesting tarot-like (top view) and crown-like (side view) views, among which one central {$K_4(UO_2)_3(H_2O)_3$} cluster was surrounded by one {α-SiW_9} and three {γ-SiW_{10}} building units. In addition, a more significant aspect is that **U_3** shows good catalytic activity in the dehydration condensation of aldehydes, acetoacetates, and urea to green synthesize dihydropyrimidin-2(1*H*)-ones. The advantages of this transformation include solvent-free conditions, water as the sole by-product, available starting materials, good compatibility, and operational simplicity.

Published on 01 February 2023. Downloaded on 01/10/2024 6:22:59 PM.

Introduction

Self-assembly of metal–oxygen clusters with definite structures makes it possible to design and synthesize metal oxide materials from micro- to macro-scale. Polyoxometalates (POMs) are a kind of molecular metal–oxygen-cluster with various structures and important properties involving applications in catalysis, photoelectric materials, medicine, *etc.*[1–9] In general, *in situ* and precursor strategies are the mainstream methods used in the synthesis of 3d/4f-metal-containing POMs. Thousands of 3d/4f-metal-containing POMs have been reported and show fascinating properties. The *in situ* method offers more driving powers to intrinsically build new POMs by adjusting the reaction steps and conditions, while the usage of lacunary POMs precursors makes it easier to predict the structures of the obtained POMs. However, the development of actinide-containing POMs may be limited by synthetic methods, and the study still lags far behind 3d/4f-metal-containing POMs comparing the research contents and depth, which includes structure-based research and applications.[10] Actinides that have unique 5f electrons and bigger atomic radii may show more abundant oxidation states and are good members to synthesize POMs.[11–16] For these stable actinides, thorium and uranium are most accessible to study, and U-containing heteropolytungstates (U-POWs) are the most explored. But it is disappointing to note that less than ten cases were *in situ* synthesized and dozens of U-POWs were all synthesized using lacunary POM precursors among these U-POWs.[17–22] Thus, the knowledge of the structural diversities of actinide-containing POMs still needs exploitation.

It should be noted that the synthesis of POMs that contain more than one lacunary POM building unit is quite challenging due to the complexity of the self-assembly. Most of the U-POWs are based on one type of building unit and there are only four cases that contain more than one type of lacunary POM building unit, named hybrid structures. The first structure reported by Pope in 2001 was $[(UO_2)_3(H_2O)_5As_3W_{29}O_{104}]^{19-}$, which consisted of a trivacant Keggin-{AsW_9} and a Dawson-like {$(AsW_9)_2(W_2)$} building units.[23] The second one, $[(UO_2)_3(H_2O)_4As_3W_{26}O_{94}]^{17-}$, was based on Keggin-{$AsW_9$} and a rare Dawson-like {$(AsW_8)_2W$} building units.[24] The third showed an iso-heteropolytungstate hybrid structure, $[(H_3Sb^{III}W_{17}O_{59})U^{IV}(HW_5O_{18})]^{11-}$, which was *in situ* constructed from simple

[a]*School of Chemistry, Biology and Material Science, Jiangxi Province Key Laboratory of Synthetic Chemistry, Jiangxi Key Laboratory for Mass Spectrometry and Instrumentation, East China University of Technology, Nanchang 330013, China. E-mail: like90@foxmail.com, erick@ecut.edu.cn*

[b]*Key Lab of Organic Optoelectronics & Molecular Engineering of Ministry of Education, Department of Chemistry, Tsinghua University, Beijing 100084, China. E-mail: yonggewei@mail.tsinghua.edu.cn*

[c]*School of Chemistry and Pharmaceutical Sciences, Guangxi Normal University, Guilin, 541000, China*

†Electronic supplementary information (ESI) available: Bond lengths/angles, tables, and additional figures. CCDC 2132862. For ESI and crystallographic data in CIF or other electronic format see DOI: https://doi.org/10.1039/d2qi02653h

‡These authors contributed equally to this work.

Published on 01 February 2023. Downloaded on 01/10/2024 6:22:59 PM.

materials with monovacant Lindqvist-{W_5} and monovacant Dawson-{SbW_{17}} building units.[18] Recently, Zhang's and our group have reported the fourth hybrid U-POW, $K_{1.5}Na_{13.25}[(UO_2)_3(SeO_3)_3Na_5(H_2O)_6(SeW_6O_{21})(SeW_9O_{33})_3]\cdot 26H_2O$, which was *in situ* synthesized with one Anderson-{SeW_6} and three Keggin-{SeW_9} building units.[22]

The usage of lacunary POM precursors indeed makes it efficient to synthesize new POMs, but the relatively strong stabilities of lacunary POM precursors also reduce the structural uncertainties of the obtained new POMs.[25–27] Thus, these changeful and relatively unstable lacunary POM precursors with low stabilities are preferred to build new U-POWs.[28–33] For example, Kortz reported a horseshoe-like U-POW, *e.g.*, $K_6Li_{19}[Li(H_2O)K_4(H_2O)_3\{(UO_2)_4(O_2)_4(H_2O)_2\}_2(PO_3OH)_2P_6W_{36}O_{136}]\cdot 74H_2O$, which was synthesized using the precursor $[H_6P_4W_{24}O_{94}]^{18-}$ ({P_4W_{24}}).[34] {P_4W_{24}} transformed into a rare {P_2W_{12}}-trimeric {P_6W_{36}} building unit in an LiAc buffer in the synthetic procedure. Another representative case is the third hybrid U-POW, $(NH_4)_{17}[(UO_2)_3(H_2O)_4As_3W_{26}O_{94}]\cdot 16H_2O$, as mentioned earlier, which was synthesized from {AsW_9} ($Na_9[AsW_9O_{33}]\cdot 27H_2O$).[24] A part of {$AsW_9$} lost another {$WO_6$} and assembled into a rare Dawson-like {$(AsW_8)_2W$} building unit. {γ-SiW_{10}} is one of the most changeful lacunary POM precursors and could undergo complicated transformations into monovacant {SiW_{11}}, trivacant {SiW_9}, and other species in solution.[35] Thus, new U-POWs may be obtained using {γ-SiW_{10}} under specific conditions.

Regarding the aforementioned cases, we report a new U-POW with hybrid polyanions: $\{K_{4.2}Na_{18.9}H_{0.9}(H_2O)_{20}[K_4(UO_2)_3(H_2O)_6(\alpha\text{-}SiW_9O_{34})(\gamma\text{-}SiW_{10}O_{36})_3]\}\cdot ca.16H_2O$ (**U_3**), which is synthesized by a one-pot method using $K_8[\gamma\text{-}SiW_{10}O_{36}]\cdot 12H_2O$ and $UO_2(OAc)_2$. A part of {γ-SiW_{10}} transformed into trivacant {α-SiW_9} in the aqueous solution and joined in the assembly of the polyanion. The polyanion of **U_3** shows a quadrahedron-like configuration based on a {$K_4(UO_2)_3(H_2O)_6$} cluster chromophore and two kinds of lacunary silicotungstate building units, *e.g.*, trivacant {α-SiW_9} and bivacant {γ-SiW_{10}}. This work provides the first case of U-POW that is constructed from two kinds of Keggin-type lacunary building units. Besides, **U_3** shows good catalytic activity in the synthesis of dihydropyrimidin-2(1*H*)-ones (DHPMs) *via* the dehydration condensation of aldehydes, acetoacetates, and urea. The solvent-free conditions, water as the sole by-product, and simple starting materials make this method suitable for the green synthesis of DHPMs.

Experimental

Materials and methods

The precursor $K_8[\gamma\text{-}SiW_{10}O_{36}]\cdot 12H_2O$ was synthesized according to the method reported by Hervéa.[36] Other reagents were purchased from the reagent manufacturers and used without further purification. CAUTION! *Although the uranyl salt used is depleted, it is still radioactive and toxic. Appropriate protective measures are still necessary for handling all radioactive materials.*

Synthesis of U_3

In a NaCl aqueous solution (0.25 M, 20 mL), $UO_2(OAc)_2\cdot 2H_2O$ (0.1 mmol, 0.0424 g) and $K_8[\gamma\text{-}SiW_{10}O_{36}]\cdot 12H_2O$ (0.4 mmol, 1.1884 g) were dissolved successively. The pH value of the mixture was then adjusted to 5.9 using 1 M HCl. The cloudy solution was heated and stirred at 85 °C for 30 min. During the heating procedure, this cloudy solution would transform from cloudy to clear and then cloudy again. After cooling down to room temperature, NaCl (4 g) was added to the solution and stirred for 5 min. The resulting solution was filtered and the filtrate was left to evaporate at room temperature. A cold room temperature (below 10 °C) is necessary for the formation of **U_3**. Unknown and cubic crystals will appear if the room temperature is higher.[37] Yellow-green crystals of **U_3** with rod-like shapes were collected after two weeks (yield: 11% based on $UO_2(OAc)_2\cdot 2H_2O$). Elemental analysis (ICP-OES, %) for $H_{84.9}K_{8.2}Na_{18.9}O_{190}Si_4U_3W_{39}$, found: Na, 3.37; K, 2.49; W, 55.68. IR (cm^{-1}): 3388 (s), 1624 (m), 1005 (w), 945 (m), 847 (vs), 787 (s), 722 (vs), 689 (vs), 558 (m).

Typical procedure of dehydration condensation reaction catalyzed by U_3

Benzaldehyde (1 mmol), ethyl acetoacetate (1.5 mmol), urea (1 mmol), and **U_3** (0.2 mol%) were added to a 4 mL reaction vial. Then the reaction was carried out at 100 °C for 3 h. After cooling down to room temperature, the crude product was dissolved in hot EtOH (10 mL). After simple filtration, the filtrate was cooled in an ice bath to promote the recrystallization of the desired product. The purified products were all characterized by NMR and the corresponding data are provided in the ESI.†

Results and discussion

Analysis of U_3

The single-crystal analysis demonstrates that **U_3** crystallizes in the $P\bar{1}$ space group. The polyanion in **U_3** consists of three parts, including one {$K_4(UO_2)_3(H_2O)_6$} chromophore at the centre of the polyanion, one {α-SiW_9} and three {γ-SiW_{10}} moieties (Fig. 1A). In the triangular {$K_4(UO_2)_3(H_2O)_6$} chromophore, all the three U(VI) atoms (U1/U2/U3) show a similar 7-coordinated distorted pentagonal bipyramidal geometry at the peak of the triangle. The polar oxygen atoms from the U(VI) pentagonal bipyramid could be divided into two groups based on the positions relative to U(VI) atoms (Fig. S1†). The bond lengths of three inner polar oxygen atoms and the corresponding U(VI) atoms (O1 for U1, O3 for U2, and O5 for U3) are in the range of 1.795(18) to 1.811(17) Å, which are slightly longer than the typical O═U═O bonds (1.75–1.79 Å), while the outside polar oxygen atoms (O2 for U1, O4 for U2 and O6 for U3) show normal U═O bond lengths (1.736(16) Å for O2–U1, 1.794(18) Å for O4–U2 and 1.781(17) for O6–U3). The bond angles for O═U═O bonds are also distorted compared with a standard uranyl ion (178.048(13)° for U1, 179.418(10)° for U2 and 178.997(11)° for U3). For the five equatorial oxygen atoms,

 This journal is © the Partner Organisations 2023

Published on 01 February 2023. Downloaded on 01/10/2024 6:22:59 PM.

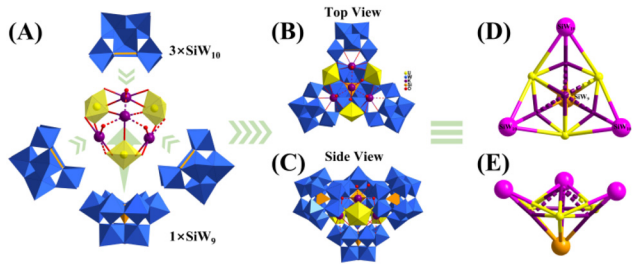

Fig. 1 (A) Schematic depiction of the units in the polyanion of U_3; (B) top view and (C) side view of the polyanion in U_3; and (D) and (E) the simplified schematic depiction of the polyanion in U_3.

four oxygen atoms coordinated with K(I) ions are offered by {α-SiW_9} and {γ-SiW_{10}}, while the other oxygen atoms (O7/O8/O9) are coordinated with water molecules. The five equatorial oxygen atoms (O7/O10/O11/O16/O17) for U1 are almost coplanar and the deviation is less than 0.05 Å. But O8 is 0.0848 Å away from the plane constructed by O12/O13/O18 for U2. For U3, the four equatorial oxygen atoms (O14/O15/O20/O21) offered by polyanions are almost coplanar and O9 is 0.1433 Å away from the plane of O14/O15/O20.

In the typical coordination bond lengths of K–O bonds (2.9 Å), K1 is coordinated by four equatorial oxygen atoms (O10/O12/O17/O18), one coordinated water molecule (O151), and two other oxygen atoms (bridging oxygen atoms offered by {γ-SiW_{10}}) (Fig. S1†). K2 is coordinated by three equatorial oxygen atoms (O14/O19/O20), one coordinated water molecule (O152), and one oxygen atom offered by {γ-SiW_{10}}. Similarly, K3 is also coordinated by three equatorial oxygen atoms (O11/O16/O21), one coordinated water molecule (O153) and the other two oxygen atoms offered by {γ-SiW_{10}}. Thus, a triangular arrangement is constructed by the connection of three U(VI) pentagonal bipyramids and three K(I) ions. K1 to K3 have weak coordination interactions with adjacent oxygen with distances from 2.9161(3) to 3.2179(3) Å. K4 is located at the position above the centre of this triangle and is coordinated by two inner polar oxygen atoms (O1/O5) from U1 and U3 with bond lengths of 2.8974(2) and 2.8993(2) Å, respectively. The distance from K4 to the plane of U1/U2/U3 is 2.3507 Å. Besides, K4 also has weak coordination interactions with adjacent oxygen atoms and two halves of water molecules (O154/O155) in the range of 2.9188(3)–3.2768(3) Å. In short, a triangular {$K_4(UO_2)_3(H_2O)_6$} chromophore is constructed dexterously by the connection of U(VI) and K(I) ions and oxygen atoms offered by {α-SiW_9} and {γ-SiW_{10}}. Three U(VI) ions are at the peaks of the triangle and K1 to K3 are located at the centre of the edges.

In addition, one {α-SiW_9} offers all the six peak oxygen atoms (O16–O21) to coordinate with three U(VI) and K(I) ions from the direction perpendicular to the plane of the triangle at the opposite side from K4. All the three {γ-SiW_{10}} building units that act as inorganic multidentate ligands only offer two terminal oxygen atoms and one or two bridging oxygen atoms to coordinate with U(VI) and K(I) ions from directions perpendicular to the edges of the triangle, respectively. Thus, the three {γ-SiW_{10}} units are all unsaturated. The plane constructed by Si2 to Si4 from three {γ-SiW_{10}} units is not parallel to the plane formed by U1 to U3; the dihedral angle is 2.768°, while the distance between K4 and plane Si2 to Si4 is only 0.0930 Å. As a result, a hybrid quadrahedron-like polyanion in U_3 is constructed dexterously from a one {α-SiW_9}, three {γ-SiW_{10}} and one {$K_4(UO_2)_3(H_2O)_6$} cluster with a formula of $[K_4(UO_2)_3(H_2O)_6(\alpha\text{-}SiW_9O_{34})(\gamma\text{-}SiW_{10}O_{36})_3]^{24-}$ (Fig. 1B–E and 2A). Besides, adjacent $[K_4(UO_2)_3(H_2O)_6(\alpha\text{-}SiW_9O_{34})(\gamma\text{-}SiW_{10}O_{36})_3]^{24-}$ ions are alternately connected by K(I) and Na(I) ions and coordinating water molecules to form a one-dimensional chain in the typical coordination bond lengths of K–O bonds (2.9 Å) and Na–O bonds (2.6 Å) (Fig. S2†).

It is worth noting that there are strong hydrogen bonds between the six coordinated water molecules (O7/O8/O9/O151/O152/O153) and six uncoordinated peak oxygen atoms (O145–O150) from three {γ-SiW_{10}} (Fig. 2B). The distances between the donors and the acceptors are in the range of 2.67(3)–3.17(3) Å (Table S4†). Twelve oxygen atoms are connected in a zigzag manner by hydrogen bonds to form a heart-like arrangement. These hydrogen bonds help stabilize the unsaturated coordination structure.

The formula of U_3 was determined by various characterization methods. The ICP-OES results reveal that the mass fractions of K, Na, and W in U_3 were 2.49%, 3.37%, and 55.68%, respectively. Thus, the number of K : Na : W should be 8.2 : 18.9 : 39 and there was 0.9 hydrogen ion for charge balance. The TGA curve of U_3 gives a 5.86% weight loss from room temperature to 300 °C, which corresponds to about 42 water molecules (Fig. S3†). The number of lattice water molecules removed by the SQUEEZE procedure is 16. Thus, the formula of U_3 should be $\{K_{4.2}Na_{18.9}H_{0.9}(H_2O)_{20}[K_4(UO_2)_3(H_2O)_6(\alpha\text{-}SiW_9O_{34})(\gamma\text{-}SiW_{10}O_{36})_3]\}\cdot ca.16H_2O$. The elementary composition of U_3 was also confirmed by energy dispersive spectroscopy (EDS) mapping results (Fig. S4†). Electrospray ionization mass spectrometry (ESI-MS) results demonstrated the chemical behaviours of U_3 in water (Fig. S5 and Table S6†). The unsaturated coordination structure of U_3 partly decomposed in electrospray ionization, but the polyanion of U_3 could also maintain a degree of stability. U_3 could be used as a catalyst under mild conditions. Besides, Fourier transform infrared, Raman, and solid-state luminescence spectra of U_3 were also recorded to assess the properties of U_3 (Fig. S7–S9†).

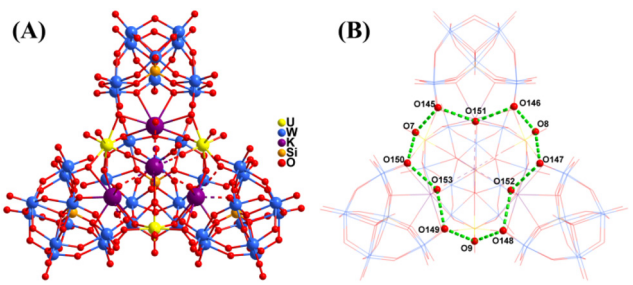

Fig. 2 (A) Ball-and-stick view of the polyanion in U_3 and (B) schematic depiction of the hydrogen bonds in U_3.

Published on 01 February 2023. Downloaded on 01/10/2024 6:22:59 PM.

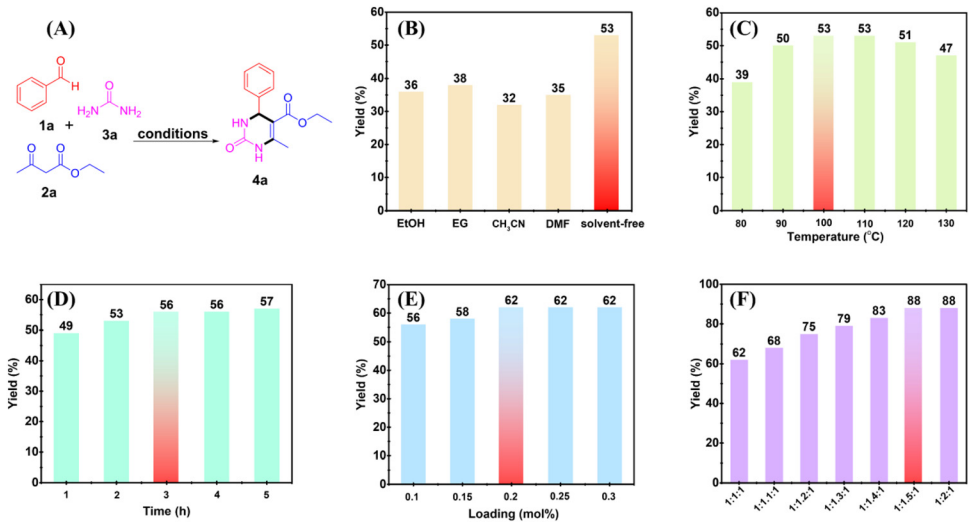

Fig. 3 (A) Model reaction: benzaldehyde (**1a**, 1 mmol), ethyl acetoacetate (**2a**, 1 mmol), urea (**3a**, 1 mmol), U_3 (0.1 mol%), solvent (1 mL), 100 °C, and 2 h; (B) screening of the reaction solvent (EG: ethylene glycol and DMF: *N*, *N*-dimethylformamide); (C and D) optimizing reaction temperature and time; (E) exploring the dosage of the catalyst; and (F) investigating the proportion of substrates (**1a** : **2a** : **3a**).

Evaluation of the catalytic activity of U_3

The evaluation of the catalytic activity of U_3 was performed in the synthesis of DHPMs through the dehydration condensation of aldehydes, acetoacetates, and urea.[37–40] DHPMs play an extremely important role in organic synthesis and pharmaceutical chemistry, and have received great attention from organic chemists.[41–45] Certain derivatives have good effects in anti-tumour, anti-inflammatory, and anti-bacterial activities, *etc.*, and especially, some functional DHPMs are considered to have great development potential in the clinical treatment of calcium channel block, adrenergic antagonism, neuropeptide Y antagonism, and so on.[46–49] This research would provide a promising catalytic system for the synthesis of DHPMs in good yields through a green method.

The reaction was carried out with benzaldehyde (**1a**), ethyl acetoacetate (**2a**), and urea (**3a**) as the model substrates, U_3 as the catalyst, and various reaction conditions were optimized including the solvent, reaction temperature and time, the dosage of the catalyst, and the proportion of substrates (Fig. 3A). From Fig. 3B, there is no doubt that the catalytic activity of U_3 is better under solvent-free conditions than in other solvents. Besides, from Fig. 3C–F, it is obvious that the product **4a** yield increases with an increase of temperature, time, the dosage of the catalyst, and the proportion of the substrates. By screening, the optimum reaction conditions of the catalytic system were obtained as follows: 0.2 mol% U_3, solvent-free, 100 °C, 3 h, and **1a** : **2a** : **3a** = 1 : 1.5 : 1.

Having established the optimal reaction conditions, the scope of this transformation was further investigated (Table 1). A range of benzaldehyde derivatives (**1**) having both electron-donating groups (*p*-Me, *m*-Me, *o*-Me, *p*-^{i}Pr, *p*-OMe, and *p*-OEt) and electron-withdrawing groups (*p*-F, *p*-Cl, *p*-Br, and *p*-N(Me)$_2$) were tested with ethyl acetoacetate (**2a**) and urea (**3a**). Generally, all the reactions proceeded smoothly with good

Table 1 Synthesis of DHPMs catalyzed by U_3 [a]

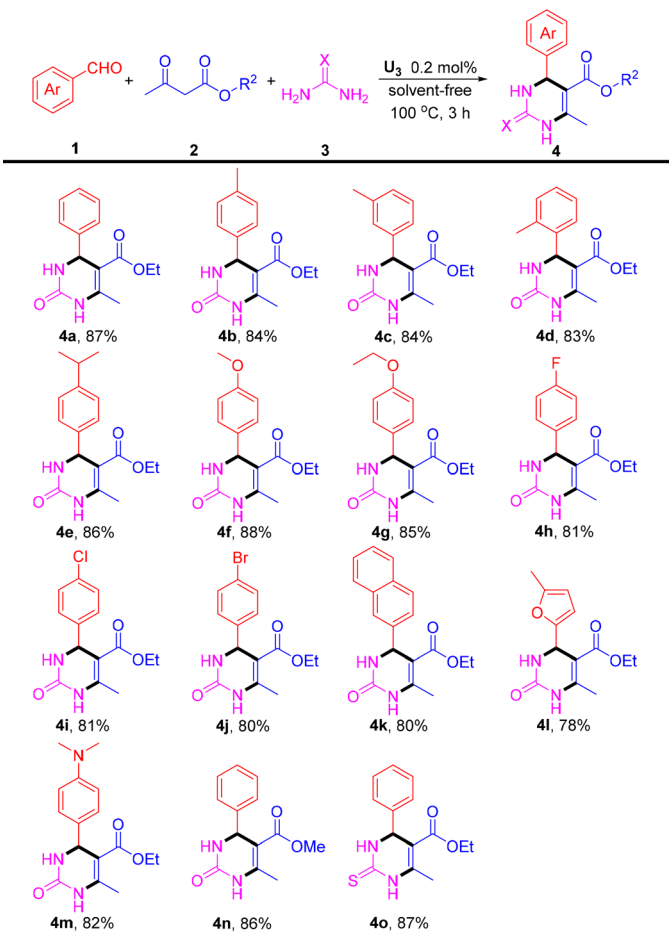

[a] Reaction conditions: benzaldehydes (**1**, 1.0 mmol), ethyl acetoacetates (**2**, 1.5 mmol), urea (**3**, 1.0 mmol), U_3 (0.2 mol%), solvent-free conditions, 100 °C, and 3 h.

This journal is © the Partner Organisations 2023

Published on 01 February 2023. Downloaded on 01/10/2024 6:22:59 PM.

yields of the corresponding products (**4b–4j**, and **4m**). In addition, it was found that 2-naphthaldehyde and 5-methyl furfural can also react with ethyl acetoacetate (**2a**) and urea (**3a**) to generate the desired products **4k** and **4l** in moderate yields. Subsequently, we studied the reaction of benzaldehyde (**1a**), methyl acetoacetate (**2b**), and urea (**3a**), giving the product **4n** in a yield of 86%. More interestingly, our protocol is applicable to the reaction of benzaldehyde (**1a**), ethyl acetoacetate (**2a**), and thiourea (**3b**), delivering the corresponding product **4o** in a yield of 87%.

Conclusions

In summary, we have synthesized and fully characterized a new hybrid U-POW based on two kinds of Keggin-type building units. A part of $\{\gamma\text{-SiW}_{10}\}$ transformed into trivacant $\{\alpha\text{-SiW}_9\}$ in the aqueous solution and joined in the assembly to access the polyanion. $\mathbf{U_3}$ represents a rare hybrid U-POW that is built based on one $\{\alpha\text{-SiW}_9\}$ and three $\{\gamma\text{-SiW}_{10}\}$ building units. Besides, $\mathbf{U_3}$ was demonstrated to be a good catalyst for the synthesis of dihydropyrimidin-2(1*H*)-ones *via* the condensation of aldehydes, acetoacetates, and urea. Importantly, the solvent-free conditions, water as the sole by-product, and available starting materials mean that this protocol provides a green and efficient multicomponent reaction for the synthesis of DHPMs. This work provides another case of rare hybrid U-POWs and the application of U-POWs in catalytic synthesis chemistry and may benefit the development of related research.

Conflicts of interest

There are no conflicts to declare.

Acknowledgements

This work was supported by the National Natural Science Foundation of China (22001034), the Jiangxi Provincial Natural Science Foundation (20212BAB213001), and the Natural Science Foundation of Guangxi (2022GXNSFGA035003).

References

1 J. C. Liu, J. W. Zhao, C. Streb and Y. F. Song, Recent advances on high-nuclear polyoxometalate clusters, *Coord. Chem. Rev.*, 2022, **471**, 214734.
2 D. J. Zang and H. Q. Wang, Polyoxometalate-based nanostructures for electrocatalytic and photocatalytic CO_2 reduction, *Polyoxometalates*, 2022, **1**, 9140006.
3 L. B. Ni, G. P. Yang, Y. Liu, Z. Wu, Z. Y. Ma, C. Shen, Z. X. Lv, Q. Wang, X. X. Gong, J. Xie, G. W. Diao and Y. G. Wei, Self-assembled polyoxometalate nanodots as bidirectional cluster catalysts for polysulfide/sulfide redox conversion in lithium–sulfur batteries, *ACS Nano*, 2021, **15**, 12222–12236.
4 Y. Q. Gu, Q. Li, D. J. Zang, Y. C. Huang, H. Yu and Y. G. Wei, Light–induced efficient hydroxylation of benzene to phenol by quinolinium and polyoxovanadate–based supramolecular catalysts, *Angew. Chem., Int. Ed.*, 2021, **60**, 13310–13316.
5 H. H. Zeng, Y. J. Qi, Z. Y. Zhang, C. T. Liu, W. J. Peng and Y. J. Zhang, Nanomaterials toward the treatment of Alzheimer's disease: Recent advances and future trends, *Chin. Chem. Lett.*, 2021, **32**, 1857–1868.
6 H. B. He, G. Wang, S. C. Chai, X. X. Li, L. Zhai, L. X. Wu and H. L. Li, Self-assembled lamellar nanochannels in polyoxometalate-polymer nanocomposites for proton conduction, *Chin. Chem. Lett.*, 2021, **32**, 2013–2016.
7 H. L. Li, M. X. Zhang, C. Lian, Z. L. Lang, H. J. Lv and G. Y. Yang, Ring-shaped polyoxometalate built by $\{Mn_4PW_9\}$ and PO_4 units for efficient visible-light-driven hydrogen evolution, *CCS Chem.*, 2020, **2**, 2095–2103.
8 Q. B. Shen, C. J. Gómez-García, W. L. Sun, X. Y. Lai, H. J. Pang and H. Y. Ma, Improving the photocatalytic H_2 evolution activity of Keggin polyoxometalates anchoring copper-azole complexes, *Green Chem.*, 2021, **23**, 3104–3114.
9 X. Guo, X. Wan, Q. T. Liu, Y. C. Li, W. W. Li and J. L. Shui, Phosphated IrMo bimetallic cluster for efficient hydrogen evolution reaction, *eScience*, 2022, **2**, 304–310.
10 G. P. Yang, K. Li and C. W. Hu, Recent advances in uranium-containing polyoxometalates, *Inorg. Chem. Front.*, 2022, **9**, 5408–5433.
11 T. Auvray and E. M. Matson, Polyoxometalate-based complexes as ligands for the study of actinide chemistry, *Dalton Trans.*, 2020, **49**, 13917–13927.
12 M. Dufaye, S. Duval and T. Loiseau, Trends and new directions in the crystal chemistry of actinide oxo-clusters incorporated in polyoxometalates, *CrystEngComm*, 2020, **22**, 3549–3562.
13 D. X. Gui, W. C. Duan, J. Shu, F. W. Zhai, N. Wang, X. X. Wang, J. Xie, H. Li, L. H. Chen, J. Diwu, Z. F. Chai and S. A. Wang, Persistent superprotonic conductivity in the order of 10^{-1} S cm^{-1} achieved through thermally induced structural transformation of a uranyl coordination polymer, *CCS Chem.*, 2019, **1**, 197–206.
14 J. Xie, Y. X. Wang, W. Liu, X. M. Yin, L. H. Chen, Y. M. Zou, J. Diwu, Z. F. Chai, T. E. Albrecht-Schmitt, G. K. Liu and S. A. Wang, Highly sensitive detection of ionizing radiations by a photoluminescent uranyl organic framework, *Angew. Chem., Int. Ed.*, 2017, **56**, 7500–7504.
15 L. W. Cheng, C. Y. Liang, W. Liu, Y. X. Wang, B. Chen, H. L. Zhang, Y. L. Wang, Z. F. Chai and S. A. Wang, Three-dimensional polycatenation of a uranium-based metal–organic cage: Structural complexity and radiation detection, *J. Am. Chem. Soc.*, 2020, **142**, 16218–16222.
16 Y. X. Wang, X. M. Yin, W. Liu, J. Xie, J. F. Chen, M. A. Silver, D. P. Sheng, L. H. Chen, J. Diwu, N. Liu, Z. F. Chai, T. E. Albrecht-Schmitt and S. A. Wang, Emergence of uranium as a distinct metal center for build-

Published on 01 February 2023. Downloaded on 01/10/2024 6:22:59 PM.

ing intrinsic X–ray scintillators, *Angew. Chem., Int. Ed.*, 2018, **57**, 7883–7887.

17 A. J. Gaunt, I. May, R. Copping, A. I. Bhatt, D. Collison, O. D. Fox, K. T. Holman and M. T. Pope, A new structural family of heteropolytungstate lacunary complexes with the uranyl, UO_2^{2+}, cation, *Dalton Trans.*, 2003, 3009–3014.

18 Y. Jeannin, Synthesis and crystallographic study of a new composite of assymetric coordination of uranium(IV) linked to two ligands of the polytungstate type $[((H_3Sb^{III}W_{17}O_{59}))U^{IV}(HW_5O_{18})]^{11-}$, *C. R. Chim.*, 2005, **8**, 999–1004.

19 R. Khoshnavazi, H. Eshtiagh-Hossieni, M. H. Alizadeh and M. T. Pope, Syntheses and structures determination of new polytungstoarsenates $[Na_2As_2W_{18}U_2O_{72}]^{12-}$ and $[MAs_2W_{18}U_2O_{72}]^{13-}$ (M = NH_4^+ and K^+), *Polyhedron*, 2006, **25**, 1921–1926.

20 H. Y. Wang, X. Y. Zheng, L. S. Long, X. J. Kong and L. S. Zheng, Sandwich-type uranyl phosphate–polyoxometalate cluster exhibiting strong luminescence, *Inorg. Chem.*, 2021, **60**, 6790–6795.

21 M. Y. Cheng, Y. F. Liu, W. X. Du, J. W. Shi, J. H. Li, H. Y. Wang, K. Li, G. P. Yang and D. D. Zhang, Two Dawson-type U(VI)-containing selenotungstates with sandwich structure and its high-efficiency catalysis for pyrazoles, *Chin. Chem. Lett.*, 2022, **33**, 3899–3902.

22 M. Y. Cheng, H. Y. Wang, Y. F. Liu, J. W. Shi, M. Q. Zhou, W. X. Du, D. D. Zhang and G. P. Yang, Bouquet-like uranium-containing selenotungstate consisting of two different Keggin-/Anderson-type units with excellent photoluminescence quantum yield, *Chin. Chem. Lett.*, 2023, **34**, 107209.

23 K.-C. Kim and M. T. Pope, New plenary and lacunary polyoxotungstate structures assembled from nonatungstoarsenate(III) anions and uranyl cations, *J. Chem. Soc., Dalton Trans.*, 2001, 986–990.

24 K.-C. Kim, A. Gaunt and M. T. Pope, New heteropolytungstates incorporating dioxouranium(VI). derivatives of α-$[SiW_9O_{34}]^{10-}$, α-$[AsW_9O_{33}]^{9-}$, γ-$[SiW_{10}O_{36}]^{8-}$, and $[As_4W_{40}O_{140}]^{28-}$, *J. Cluster Sci.*, 2002, **13**, 423–436.

25 Y. Koizumi, K. Yonesato, K. Yamaguchi and K. Suzuki, Ligand-protecting strategy for the controlled construction of multinuclear copper cores within a ring-shaped polyoxometalate, *Inorg. Chem.*, 2022, **61**, 9841–9848.

26 H. F. Li, W. J. Chen, Y. J. Zhao, Y. Zou, X. Zhao, J. P. Song, P. T. Ma, J. Y. Niu and J. P. Wang, Regulating the catalytic activity of multi-Ru-bridged polyoxometalates based on differential active site environments with six-coordinate geometry and five-coordinate geometry transitions, *Nanoscale*, 2021, **13**, 8077–8086.

27 J. Goura, A. Sundar, B. S. Bassil, G. Ćirić-Marjanović, D. Bajuk-Bogdanović and U. Kortz, Peroxouranyl-containing W_{48} wheel: synthesis, structure, and detailed infrared and Raman spectroscopy study, *Inorg. Chem.*, 2020, **59**, 16789–16794.

28 J. H. Liu, R. T. Zhang, J. Zhang, D. Zhao, X. X. Li, Y. Q. Sun and S. T. Zheng, A series of 3D porous lanthanide-substituted polyoxometalate frameworks based on rare hexadecahedral $\{Ln_6W_8O_{28}\}$ heterometallic cage-shaped clusters, *Inorg. Chem.*, 2019, **58**, 14734–14740.

29 J. C. Jiao, X. M. Yan, S. Z. Xing, T. Zhang and Q. X. Han, Design of a polyoxometalate-based metal–organic framework for photocatalytic C(sp^3)–H oxidation of toluene, *Inorg. Chem.*, 2022, **61**, 2421–2427.

30 L. B. Ni, H. J. Xu, H. F. Li, H. X. Zhao and G. W. Diao, 3D-Architecture via self-assembly of Krebs-type polyoxometalate $\{[Na_{10}(H_2O)_{26}][Sb_2W_{20}Zn_2O_{20}(H_2O)_6]\}$, *Polyhedron*, 2018, **155**, 59–65.

31 P. Y. Zhang, Y. L. Wang, L. Y. Yao and G. Y. Yang, Hepta-Zr-incorporated polyoxometalate assembly, *Inorg. Chem.*, 2022, **61**, 10410–10416.

32 H. L. Li, C. Lian and G. Y. Yang, $\{Ti_6\}$/$\{Ti_{10}\}$ Wheel cluster substituted silicotungstate aggregates, *Inorg. Chem.*, 2021, **60**, 16852–16859.

33 H. L. Li, C. Lian and G. Y. Yang, A ring-shaped 12-Ti-substituted poly(polyoxometalate): synthesis, structure, and catalytic properties, *Sci. China: Chem.*, 2022, **65**, 892–897.

34 S. S. Mal, M. H. Dickman and U. Kortz, Actinide polyoxometalates: incorporation of uranyl–peroxo in U–shaped 36-tungsto-8-phosphate, *Chem. – Eur. J.*, 2008, **14**, 9851–9855.

35 J. Cao, C. Liu and Q. D. Jia, Complex solution chemistry behind the simple "one–pot" synthesis of vanadium–substituted polyoxometalates unraveled by electrospray ionization mass spectrometry, *Rapid Commun. Mass Spectrom.*, 2016, **30**, 14–19.

36 A. Téazéa, G. Hervéa, R. G. Finke and D. K. Lyon, α–, β–, and γ–Dodecatungstosilicic acids: isomers and related lacunary compounds, *Inorg. Synth.*, 1990, **27**, 85–96.

37 K. Li, X. L. Lin, K. Zeng, X. F. Gao, W. Cen, Y. F. Liu and G. P. Yang, Effect of Na(I)-H_2O clusters on self-assembly of sandwich-type U(VI)-containing silicotungstates and the efficient catalytic activity for the synthesis of substituted phenylsulfonyl-1*H*-pyrazoles, *Tungsten*, 2022, **4**, 149–157.

38 G. P. Yang, X. L. Zhang, Y. F. Liu, D. D. Zhang, K. Li and C. W. Hu, Self-assembly of Keggin-type U(VI)-containing tungstophosphates with a sandwich structure: an efficient catalyst for the synthesis of sulfonyl pyrazoles, *Inorg. Chem. Front.*, 2021, **8**, 4650–4656.

39 X. Q. Huang, Y. N. Cui, J. H. Zhou, Y. L. Zhang, G. D. Shen, Q. X. Yao, J. K. Li, Z. C. Xue and G. P. Yang, Self-assembly of three Ag-polyoxovanadates frameworks for their efficient construction of CN bond and detoxification of simulant sulfur mustard, *Chin. Chem. Lett.*, 2022, **33**, 2605–2610.

40 J. Zhou, T. Yu, K. Li, K. Zeng, G. P. Yang and C. W. Hu, Two U(VI)-containing silicotungstates with sandwich structures: lewis acid–base synergistic catalyzed synthesis of benzodiazepines and pyrazoles, *Inorg. Chem.*, 2022, **61**, 3050–3057.

41 M. Aslam and S. Verma, Biological activity of newly synthesized substituted dihydropyrimidinone and thione, *Int. J. ChemTech Res.*, 2012, **4**, 109–111.

 This journal is © the Partner Organisations 2023

Published on 01 February 2023. Downloaded on 01/10/2024 6:22:59 PM.

42 L. Saher, M. Makhloufi-Chebli, L. Dermeche, B. Boutemeur-Khedis, C. Rabia, A. M. S. Silva and M. Hamdi, Keggin and Dawson-type polyoxometalates as efficient catalysts for the synthesis of 3,4-dihydropyrimidinones: experimental and theoretical studies, *Tetrahedron Lett.*, 2016, **57**, 1492–1496.
43 S. Rezayati, F. Kalantari, A. Ramazani, S. Sajjadifar, H. Aghahosseini and A. Rezaei, Magnetic silica-coated picolylamine copper complex [Fe_3O_4@SiO_2@GP/picolylamine-Cu(II)]-catalyzed Biginelli annulation reaction, *Inorg. Chem.*, 2021, **61**, 992–1010.
44 W. G. Fan, Y. Queneau and F. Popowycz, HMF in multicomponent reactions: utilization of 5-hydroxymethylfurfural (HMF) in the Biginelli reaction, *Green Chem.*, 2018, **20**, 485–492.
45 P. Noppawan, S. Sangon, N. Supanchaiyamat and A. J. Hunt, Vegetable oil as a highly effective 100% bio-based alternative solvent for the one-pot multicomponent Biginelli reaction, *Green Chem.*, 2021, **23**, 5766–5774.
46 S. R. Kumar, A. Idhayadhulla, A. J. A. Nasser and J. Selvin, Synthesis and antimicrobial activity of a new series 1,4-dihydropyridine derivatives, *J. Serb. Chem. Soc.*, 2011, **76**, 1–11.
47 J. Lloyd, H. J. Finlay, W. Vacarro, T. Hyunh, A. Kover, R. Bhandaru, L. Yan, K. Atwal, M. L. Conder and T. Jenkins-West, Pyrrolidine amides of pyrazolodihydropyrimidines as potent and selective Kv1.5 blockers, *Bioorg. Med. Chem. Lett.*, 2010, **20**, 1436–1439.
48 Â. de Fátima, T. C. Braga, L. d. S. Neto, B. S. Terra, B. G. F. Oliveira, D. L. da Silva and L. V. Modolo, A mini-review on biginelli adducts with notable pharmacological properties, *J. Adv. Res.*, 2015, **6**, 363–373.
49 C. O. Kappe, Biologically active dihydropyrimidones of the biginelli-type—a literature survey, *Eur. J. Med. Chem.*, 2000, **35**, 1043–1052.